*Journal of Physiology* (1989), **412**, *pp.* 181–195
*With 10 text-figures*
*Printed in Great Britain*



# DIHYDROPYRIDINE-SENSITIVE LOW-THRESHOLD CALCIUM CHANNELS IN ISOLATED RAT HYPOTHALAMIC NEURONES

BY N. AKAIKE, P. G. KOSTYUK* AND Y. V. OSIPCHUK*

*From the Department of Neurophysiology, Tohoku University, School of Medicine, Sendai 980, Japan*

(*Received 30 June 1988*)

SUMMARY

1. Low-voltage-activated $Ca^{2+}$ channels which produce a transient inward current were studied in neurones freshly isolated from the ventromedial hypothalamic region of the rat. Membrane currents were recorded using a suction-pipette technique which allows for internal perfusion under a single-electrode voltage clamp. A concentration-jump technique was also used for rapid drug application.

2. In most cells superfused with 10 mM-$Ca^{2+}$, a transient inward $Ca^{2+}$ current was evoked by a step depolarization to potentials more positive than −65 mV from a holding potential of −100 mV. Such a low-threshold $Ca^{2+}$ current could easily be separated from a high-threshold, steady type of $Ca^{2+}$ current by selecting the holding and test potential levels, as well as by resistance to the wash-out during cell dialysis.

3. Activation and inactivation processes of the low-threshold $Ca^{2+}$ current were highly potential dependent at 20–22 °C. For a test potential change from −60 to +20 mV, the time to peak of the current decreased from 45 to 9 ms, and the time constant of the current decay decreased from 90 to 40 ms. The steady-state inactivation occurred at very negative potentials, reaching a 50% level at −93 mV. Recovery from inactivation showed a time constant between 2·63 and 0·94 s for a potential change from −80 to −120 mV.

4. The amplitude of the low-threshold $Ca^{2+}$ current depended on the external $Ca^{2+}$ concentration ($[Ca^{2+}]_o$), approaching saturation at 100 mM $[Ca^{2+}]_o$. $Ba^{2+}$ substituted for $Ca^{2+}$ reduced the current amplitude by 30–50% while $Sr^{2+}$ produced no definite changes in the current amplitude.

5. The low-threshold $Ca^{2+}$ current was blocked by various di- or trivalent cations in the sequence of $La^{3+} > Zn^{2+} > Cd^{2+} > Ni^{2+} > Co^{2+}$. The corresponding apparent dissociation constants ($K_D$) were $7 \times 10^{-7}$, $1 \times 10^{-4}$, $3 \times 10^{-4}$, $6 \times 10^{-4}$ and $3 \times 10^{-3}$ M.

6. Various organic $Ca^{2+}$ antagonists were effective in blocking the low-threshold $Ca^{2+}$ current in the following sequence: flunarizine > nicardipine > nifedipine > nimodipine > D600 (methoxyverapamil) > diltiazem. The corresponding $K_D$s were $7 \times 10^{-7}$, $3{\cdot}5 \times 10^{-6}$, $5 \times 10^{-6}$, $7 \times 10^{-6}$, $5 \times 10^{-5}$ and $7 \times 10^{-5}$ M. These $Ca^{2+}$ antagonists induced a use-dependent decrease in the current amplitude. Bay K 8644 blocked the

* Present address: Bogomoletz Institute of Physiology, Bogomoletz str. 4, 252601 GSP, Kiev 24, USSR.

current in a manner similar to that seen with other dihydropyridine derivatives. We conclude from this study that pharmacological properties of low-threshold $Ca^{2+}$ channels in CNS neurones differ from those in peripheral neurones.

## INTRODUCTION

The existence of voltage-sensitive $Ca^{2+}$ channels activated by a small depolarization from the cell resting potential has been evidenced mainly using peripheral excitable cells (dorsal root ganglion neurones of rat and chick: Veselovsky & Fedulova, 1982; Carbone & Lux, 1984*a*, *b*; Bossu, Feltz & Thomann, 1985; Fedulova, Kostyuk & Veselovsky, 1985; dog and frog atrial cells: Bean, 1985; guinea-pig ventricle cells: Nilius, Hess, Lansman & Tsien, 1985; Mitra & Morad, 1986; rat mesenteric artery smooth muscle: Bean, Sturek, Puga & Hermsmeyer, 1985; rat venous smooth muscle: Sturek & Hermsmeyer, 1986) and cultured cell lines (neuroblastoma cells: Narahashi, Tsunoo & Yoshii, 1987; $GH_3$ and $GH_4$ cells: Armstrong & Matteson, 1985; Cohen & McCarthy, 1985). Such low-threshold $Ca^{2+}$ channels reveal specific properties different from those in the 'classical' high-threshold $Ca^{2+}$ channels. They inactivate rapidly in a potential-dependent manner and remain functioning during intracellular perfusion or even in isolated membrane patches. They differ also in sensitivity to organic $Ca^{2+}$ channel antagonists and agonists (Boll & Lux, 1985; Fox, Nowycky & Tsien, 1987*a*).

The first finding of the presence of two different types of $Ca^{2+}$ conductances in brain neurones was in slices of the inferior olive using current-clamp techniques (Llinás & Yarom, 1981*a*). Preliminary data on the low-threshold $Ca^{2+}$ channels in brain neurones were obtained using isolated rat hippocampal cells (Gray & Johnston, 1986). However, a systematic study of this type of $Ca^{2+}$ channel in brain neurones has apparently not been documented. Using neurones freshly isolated from the rat hypothalamus, we found that these brain neurones have low-threshold $Ca^{2+}$ channels and that the pharmacological properties differ from those observed in peripheral neurones.

## METHODS

*Cell isolation.* Single neurones were isolated from ten to fifteen day-old rats (Kaneda, Nakamura & Akaike, 1988). The brain was removed from rats anaesthetized with ether and dissected into slices (about 500 $\mu$m thick) using a razor blade. The slices containing the ventromedial hypothalamic region were selected and pre-incubated in normal external solution with constant oxygenation for 20 min at 37 °C. After pre-incubation they were transferred into an external solution containing 1 mg/ml collagenase and 1 mg/ml trypsin, in which they were kept for 40 min under constant oxygenation at 37 °C. The hypothalamic region was then removed by punching and was dispersed by pipetting. Isolated cells were kept in an external solution containing 20% bovine serum and were viable for electrophysiological studies up to 12 h after dissection.

*Cell perfusion.* Selected neurones were transferred into an experimental chamber and drawn into the opening of a glass pipette (2–3 $\mu$m in diameter) filled with the internal solution described below. The membrane patch in the opening was destroyed by negative pressure pulses, and soluble cell contents were exchanged with the pipette-filling solution by diffusion.

*Current recording.* Transmembrane currents were recorded using a patch-clamp amplifier type EPC-7 L/M (List, FRG), low-pass filtered at 10 kHz, digitized at 100 kHz by a 12-bit analog-to-digital converter ADX-98 (Canopus, Japan), and stored in a 16-bit microcomputer PC 98XL (NEC, Japan). The computer was also used to control the membrane potential and the electromagnetic

value regulating the external solution exchange (Akaike, Yakushiji, Tokutomi & Carpenter, 1987), as well as to analyse the data.

*Solutions.* Standard external solution (in mM): choline chloride, 140; CsCl, 5; $CaCl_2$, 10; $MgCl_2$, 1; glucose, 10; HEPES–Tris-OH 10; pH 7·4. We used two different internal solutions (in mM): (1) *N*-methyl-D-glucamine fluoride (NMG-F), 100; tetraethylammonium chloride (TEA-Cl), 20; HEPES–NMG-OH, 10; pH 7·3; (2) caesium aspartate, 100; TEA-Cl, 20; HEPES–CsOH, 10; EGTA–$CaCl_2$, 1; pH 7·2. The free-$Ca^{2+}$ concentration of the latter internal solution buffered with $Ca^{2+}$–EGTA was calculated using the following equation:

$$\text{added } Ca^{2+} = \frac{1+K'\{[\text{EGTA}]+[Ca^{2+}]\}}{1+[Ca^{2+}]K'}[Ca^{2+}],$$

where $[Ca^{2+}]$ represents the free-$Ca^{2+}$ concentration, [EGTA] the concentration of EGTA, and $K'$ is an apparent association constant for $Ca^{2+}$–EGTA of $10^{7\cdot1}$ at pH 7·2 and 22 °C (Portzehl, Caldwell & Rüegg, 1964). We added 0·28 mM-$CaCl_2$ to the internal medium containing 1 mM-EGTA so that the free-$Ca^{2+}$ concentration would be $3\times10^{-8}$ M. All experiments were carried out at room temperature (20–22 °C).

*Drugs.* Drugs used in the experiments were: collagenase type I (Sigma), trypsin (Sankyo), flunarizine (Kyowa Hakko), nicardipine (Yamanouchi), D600 (Knoll), diltiazem (Tanabe), nimodipine, nifedipine and Bay K 8644 (Bayer). All drugs were applied to the isolated neurones by a rapid concentration jump termed as 'concentration-clamp' technique which enables an exchange of the external solution within a few milliseconds (Akaike, Inoue & Krishtal, 1986). The data were analysed statistically by Student's *t* test. The numerical values are given as mean ± S.E.M.

## RESULTS

### *Potential- and time-dependent characteristics of the low-threshold $Ca^{2+}$ current*

In $Na^+$- and $K^+$-free standard saline containing 10 mM-$Ca^{2+}$, a transient $Ca^{2+}$ inward current could be induced in most neurones by a 200 ms step depolarization to about −65 mV from a holding potential ($V_H$) of −100 mV. The current increased in amplitude with increasing depolarization, reaching a peak at about −30 mV. In about 50% of the cells, a steady $Ca^{2+}$ inward current joined to the transient one at potentials more positive than −30 mV. This high-threshold $Ca^{2+}$ current was much less stable and usually disappeared within 20 min after the start of the dialysis. In only a few cells was the low-threshold transient $Ca^{2+}$ current not detectable and the high-threshold steady $Ca^{2+}$ current appeared in a pure form.

Figure 1*A* shows typical current recordings from one of the cells at various depolarizations at a $V_H$ of −100 mV where both transient and steady $Ca^{2+}$ currents were present. In Fig. 1*B*, the corresponding current–voltage (*I–V*) curves are plotted for the current amplitude at the peak (○) and at the end (●) of the 200 ms pulse. The *I–V* curves in Fig. 1*C* and *D* demonstrate extreme data obtained from two other cells: one (*C*) showed only the low-threshold transient current component (low-voltage-activated $Ca^{2+}$ current, $I_{Ca,\,LVA}$) and the other (*D*) only the high-threshold steady current (high-voltage-activated $Ca^{2+}$ current, $I_{Ca,\,HVA}$). In addition, the ratio of amplitude between low- and high-threshold $Ca^{2+}$ currents varied from cell to cell. As will be shown later, both these currents were abolished in the presence of $Ca^{2+}$ channel blocking agents. Therefore, they represent $Ca^{2+}$ currents flowing through 'low-' and 'high-threshold' $Ca^{2+}$ channels.

The kinetic properties of the low-threshold $Ca^{2+}$ current were analysed by measuring the activation time (time to peak) and the inactivation time (decay time constant), at different testing potentials. Figure 2 illustrates representative $Ca^{2+}$

current recordings used for the kinetic analysis. In the figure, the current decay could be fitted by a sum of two exponents: the fast exponent describing the decay of the transient component and the slow exponent, the decay of the steady component. In column *A*, a recording was made every 5 s at the beginning of the experiment, a time when both low- and high-threshold $Ca^{2+}$ currents were present. Stimulation was then

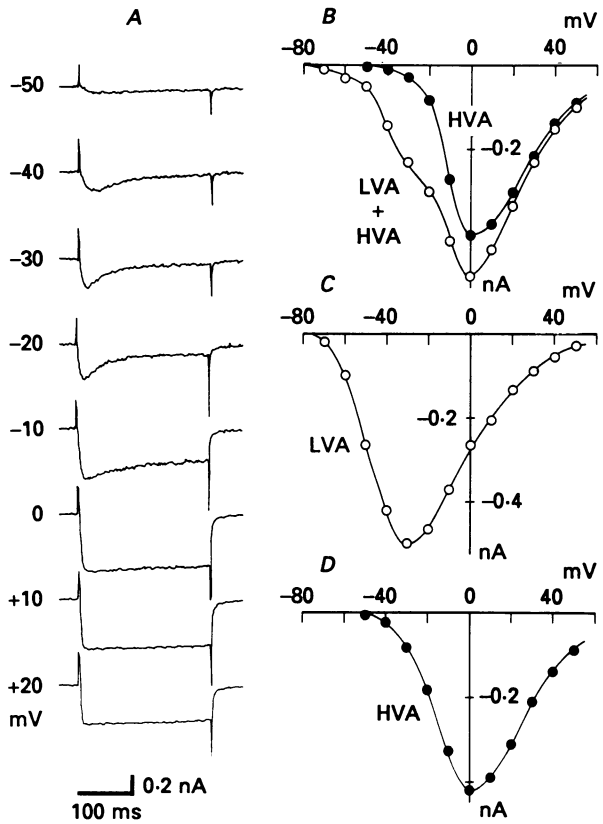


Fig. 1. $Ca^{2+}$ currents from isolated rat hypothalamic neurones. *A*, examples of current recordings at testing potentials indicated. *B*, *I–V* curves from the same cell plotted according to maximum current amplitudes (○) and their amplitudes at the end of 200 ms depolarizing pulses (●) showing the high-threshold current component. *C*, *I–V* curve from another cell in which no high-threshold $Ca^{2+}$ current was present. *D*, *I–V* curve from a third cell without low-threshold $Ca^{2+}$ current. Holding potential ($V_H$) in all cases was −100 mV. LVA, low-voltage-activated current. HVA, high-voltage-activated current.

applied for several minutes and the steady component (inset) disappeared. Column *B* presents the low-threshold $Ca^{2+}$ currents isolated in this manner. The currents were recorded from the same cell 10 min after obtaining the first record. Now the decay could be described by a single exponent with a time constant identical to that of the fast exponent in the corresponding record of column *A*. In Fig. 3 the time to peak ($t_p$) and the decay time constant ($\tau_h$) of the low-threshold $Ca^{2+}$ current are plotted against the membrane potential ($V_m$). As can be seen, both activation and inactivation of the low-threshold $Ca^{2+}$ currents are strongly potential dependent, the responses

becoming more rapid with increasing depolarization, in a manner similar to that of other ionic channels with a potential-dependent inactivation.

The steady-state inactivation of the low-threshold $Ca^{2+}$ current was measured using a 1 s pre-pulse to various potentials from −120 to −60 mV. The obtained $h_\infty$–$V_m$ curve is presented in Fig. 4, with a 0·5 value at −93 mV. In this figure the

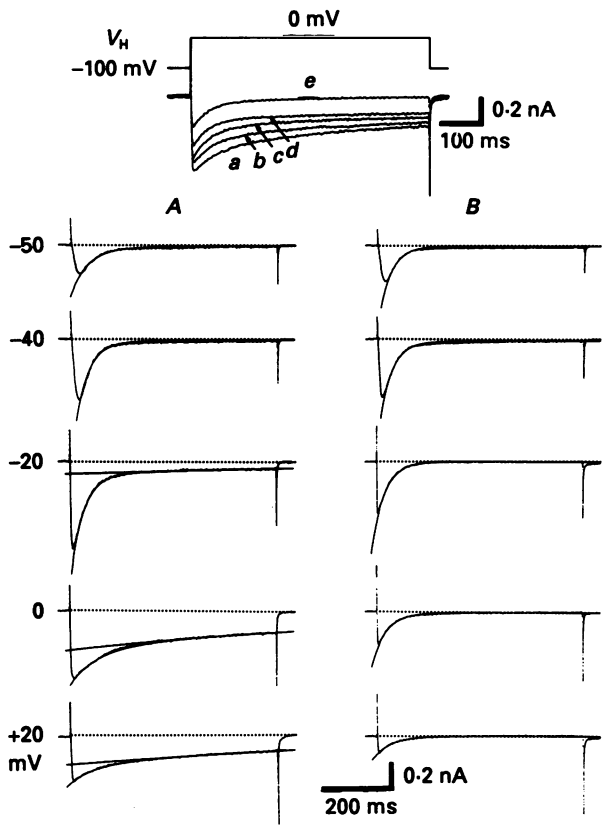


Fig. 2. Time course of inactivation decay of $Ca^{2+}$ currents. *A*, records taken at start of the experiment on a single cell together with fittings of current decay by the sum of two exponents. The cell was repeatedly stimulated for several minutes and the steady component of the current disappeared (see inset). In the inset, *a*, *b*, *c*, *d* and *e* were recorded 2, 3, 4, 5 and 10 min after the first recording of $Ca^{2+}$ current. *B*, records from the same cell after wash-out of the high-threshold $Ca^{2+}$ current component showing the monoexponential time course of inactivation. $V_H$ in all cases was −100 mV.

activation curve obtained from the same cell is also plotted. The maximum activation level was assumed to be the value extrapolated from the linear part of the *I–V* curve.

The recovery from steady-state inactivation was tested at different repolarization potentials ($V_t$) as a function of time. It showed a definite potential dependence, as can be seen in Fig. 5. In this case, the low-threshold $Ca^{2+}$ current was inactivated initially by a 3 s depolarizing pulse to −30 mV. The time course of recovery at −120, −100 or −80 mV was then monitored by a depolarizing pulse to −30 mV. Figure 5*A*

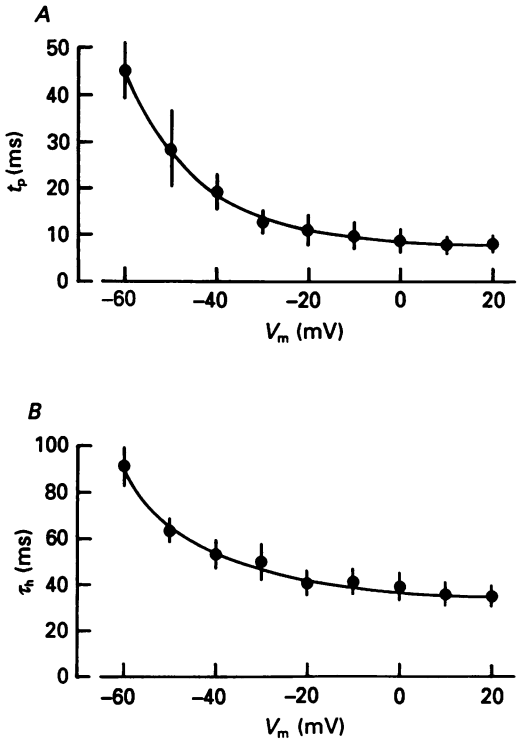


Fig. 3. Potential dependence of activation time (*A*) and inactivation velocity (*B*) of the low-threshold $Ca^{2+}$ current. Activation time was measured as the time to peak current ($t_p$), inactivation velocity as the time constant of the exponential current decay ($\tau_h$). Mean values and ±S.E.M. from measurements on five cells. $V_m$, membrane potential. $V_H$ in all cases was −100 mV.

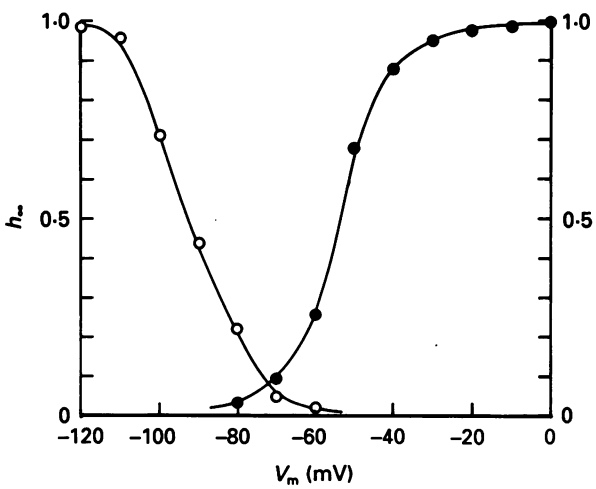


Fig. 4. Steady-state inactivation (○) and activation (●) curves for the low-threshold $Ca^{2+}$ current measured in one cell. Inactivation was induced by 1 s potential displacements before testing depolarization to −30 mV. Activation was extrapolated from the linear part of the *I–V* curve for the low-threshold $Ca^{2+}$ current.

presents responses obtained by repolarization to −120 mV, and Fig. 5*B* shows the time course of recovery at the various potential levels indicated above. The recovery could be approximated by a single exponent with time constants of 0·94 s (*a*, $V_t$ = −120 mV), 1·82 s (*b*, $V_t$ = −100 mV) or 2·63 s (*c*, $V_t$ = −80 mV).

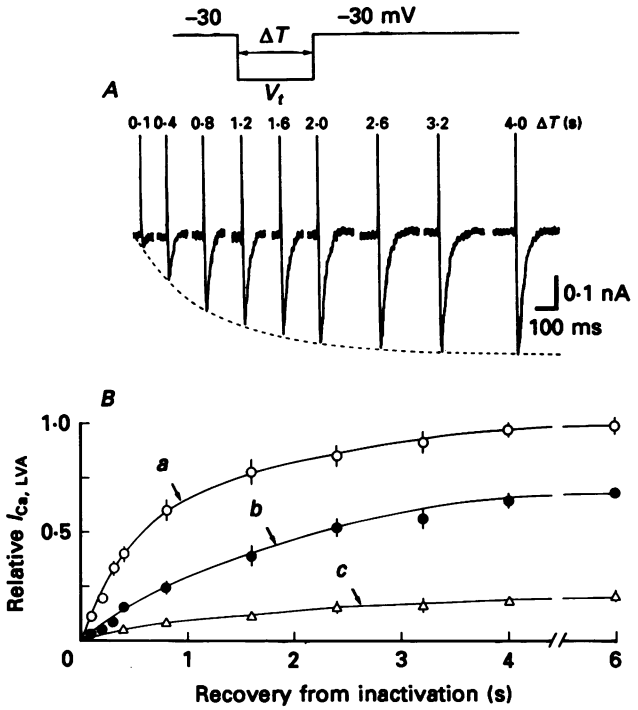


Fig. 5. Recovery from inactivation of the low-threshold $Ca^{2+}$ current. ($I_{Ca, LVA}$). *A*, examples of current records obtained in one cell by testing depolarizing pulses applied at different intervals ($\Delta T$) after the end of a 3 s membrane depolarization to −30 mV. Repolarization potential ($V_t$) −120 mV. *B*, time course of recovery at different repolarization potentials: −120 mV (○), −100 mV (●) and −80 mV (△). Time constants *a*, *b* and *c* of exponential recovery for the curves are 0·94, 1·82 and 2·63 s, respectively.

*Ionic dependence of the low-threshold $Ca^{2+}$ current*

To study the ionic dependence of the low-threshold $Ca^{2+}$ current, the amount of $Ca^{2+}$ ($CaCl_2$) in the external solution ($[Ca^{2+}]_o$) was increased at the expense of choline (choline chloride), or $Ca^{2+}$ was replaced by other divalent cations.

The relationship between $[Ca^{2+}]_o$ and amplitude of the low-threshold $Ca^{2+}$ current is shown in Fig. 6. Figure 6*A* presents the currents recorded at 10 mM (left) or 100 mM $[Ca^{2+}]_o$ (right), where the test pulses were changed from −60 to 0 mV (left) or from −50 to +20 mV (right) at a $V_H$ of −100 mV. The *I–V* curves for various $[Ca^{2+}]_o$ are plotted in Fig. 6*B*. They show a voltage shift in the positive direction with an increase in $[Ca^{2+}]_o$, which was about 20 mV for a 10-fold increase in $[Ca^{2+}]_o$. The voltage shift was presumably caused by surface-negative charges around the $Ca^{2+}$ channels (Ohmori & Yoshii, 1977).

When the peak current amplitude was plotted against various levels of $[Ca^{2+}]_o$, a clear trend towards saturation was observed but the saturation was not complete at 100 mM $[Ca^{2+}]_o$ (Fig. 6*C*). Approximately 50% saturation occurred at 10 mM $[Ca^{2+}]_o$.

After substitution of extracellular $Ca^{2+}$ with $Sr^{2+}$ or $Ba^{2+}$, the conditions for current recording became unfavourable, mainly because of a gradual increase in the

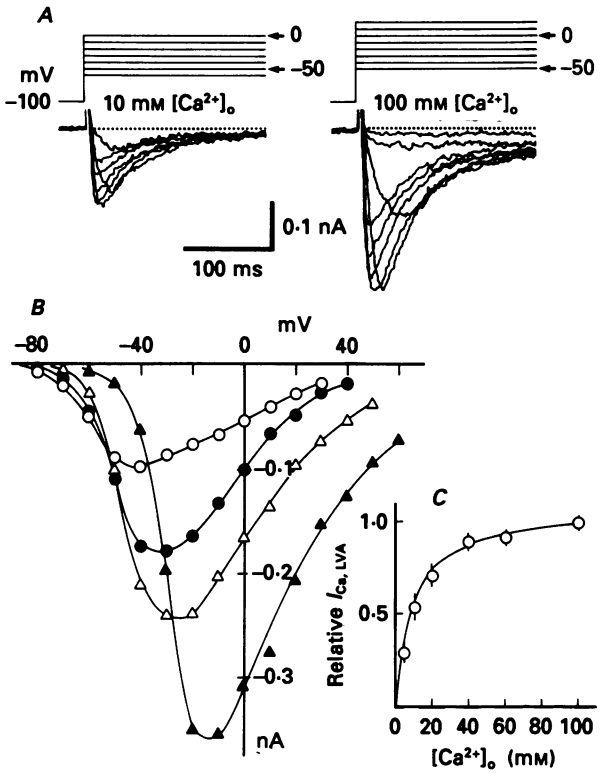


Fig. 6. Dependence of low-threshold $Ca^{2+}$ current on external $Ca^{2+}$ concentration ($[Ca^{2+}]_o$). *A*, superimposed current traces recorded from the same cell at 10 (left) and 100 (right) mM $[Ca^{2+}]_o$. Records were taken at depolarizing steps from −60 to 0 mV (left) and from −50 to +20 mV (right) at a $V_H$ of −100 mV. *B*, *I–V* curves obtained for the same cell at 5 (○), 10 (●), 20 (△) and 100 (▲) mM $[Ca^{2+}]_o$. *C*, relationship between low-threshold $Ca^{2+}$ current ($I_{Ca,\,LVA}$) and $[Ca^{2+}]_o$.

membrane leakage current. Nevertheless, in some cases, the recording condition was stable enough to compare the low-threshold $Ca^{2+}$ current with those carried by $Sr^{2+}$ and $Ba^{2+}$. After $Ba^{2+}$ substitution, the maximal amplitude of current decreased reversibly, as is shown in Fig. 7*A*. The decrease varied from 30 to 50% in different cells. The effect of substitution by $Sr^{2+}$ was less obvious; in some cells, the current amplitude became slightly augmented (Fig. 7*B*). Considering the different effects of these divalent cations on the membrane surface charge, the maximum peak currents in individual *I–V* curves in the presence of $Ca^{2+}$, $Ba^{2+}$ and $Sr^{2+}$ were compared. Even in this case, the current amplitude was in the order $I_{Sr} \geqslant I_{Ca} > I_{Ba}$. The results indicate that low-threshold current could be carried by $Ca^{2+}$, $Sr^{2+}$ or $Ba^{2+}$ but $Ca^{2+}$ was the most effective in maintaining channel activities.

*Effects of $Ca^{2+}$ antagonists on low-threshold $Ca^{2+}$ current*

Other divalent and trivalent cations known as $Ca^{2+}$ channel blockers were tested with respect to their action on the low-threshold $Ca^{2+}$ current at a $V_H$ of $-100$ mV. Recordings were made every 5 s, with or without $Ca^{2+}$ channel blockers, and the data are summarized in Fig. 8*A*. The concentration range of the polyvalent metal ions

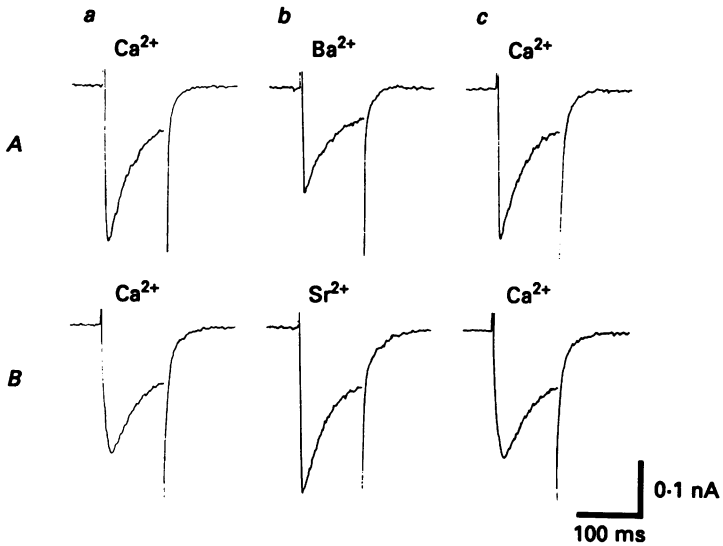


Fig. 7. Changes in low-threshold $Ca^{2+}$ current after substitution of external $Ca^{2+}$ by $Ba^{2+}$ (*A*) and $Sr^{2+}$ (*B*). $V_H$, $-100$ mV; testing pulse, $-30$ mV; ion concentration, 10 mM. Record sequence: *a*, control; *b*, substitution; *c*, control.

which exert blocking actions was in the sequence of $La^{3+} > \gg Zn^{2+} > Cd^{2+} > Ni^{2+} > Co^{2+}$. The dose–response relationships for all the ions tested followed the Langmuir adsorption isotherms with apparent $K_D$ values of $7 \times 10^{-7}$ M ($La^{3+}$), $1 \times 10^{-4}$ M ($Zn^{2+}$), $3 \times 10^{-4}$ M ($Cd^{2+}$), $6 \times 10^{-4}$ M ($Ni^{2+}$) and $3 \times 10^{-3}$ M ($Co^{2+}$). The effects of these inorganic $Ca^{2+}$ channel blockers were completely reversible.

A large variety of organic compounds known as $Ca^{2+}$ channel antagonists were also tested on the low-threshold $Ca^{2+}$ current. These currents were induced by a 200 ms step depolarization to $-30$ mV from a $V_H$ of $-100$ mV, every 5 s. The experiments were performed in the external solution containing 10 mM-$Ca^{2+}$. The compounds were diltiazem (Dil); D600; several dihydropyridine derivatives such as nimodipine (Nim), nifedipine (Nif), nicardipine (Nic), Bay K 8644; and flunarizine (Flu). The maximum inhibition of the organic $Ca^{2+}$ channel blockers on the low-threshold $Ca^{2+}$ current was observed within 1 min after application of the antagonists, as shown in Fig. 9. The steady-state inhibition to respective concentration of antagonists was then measured. The order of blocking efficiency was flunarizine > nicardipine > nifedipine > nimodipine > D600 > diltiazem (Fig. 8*B*). The apparent $K_D$ values were $7 \times 10^{-7}$ M (flunarizine), $3{\cdot}5 \times 10^{-6}$ M (nicardipine), $5 \times 10^{-6}$ M (nifedipine), $7 \times 10^{-6}$ M (nimodipine), $5 \times 10^{-5}$ M (D600) and $7 \times 10^{-5}$ M (diltiazem). No potentiating

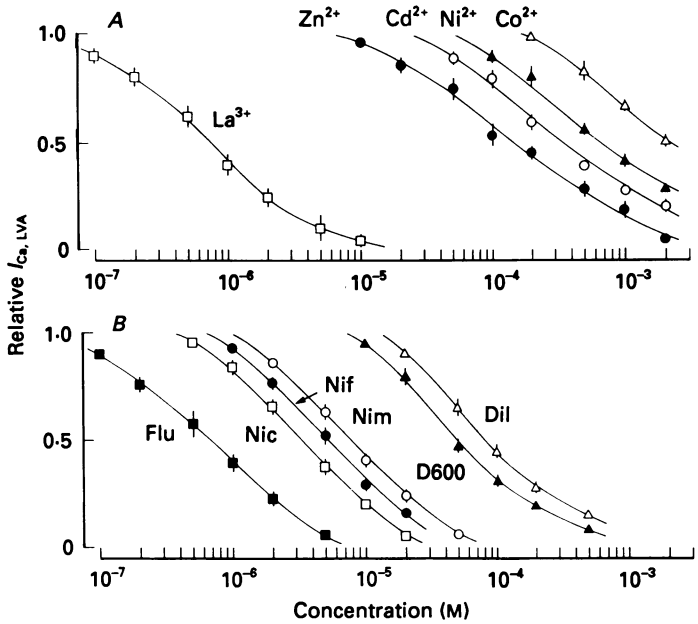


Fig. 8. Action of inorganic (*A*) and organic (*B*) blockers on low-threshold $Ca^{2+}$ current ($I_{Ca,LVA}$). The currents were induced by a 200 ms step depolarization to −30 mV from a $V_H$ of −100 mV every 5 s. *A*, effects of $Co^{2+}$, $Ni^{2+}$, $Cd^{2+}$, $Zn^{2+}$ and $La^{3+}$; *B*, effects of diltiazem (Dil), D600, nimodipine (Nim), nifedipine (Nif), nicardipine (Nic) and flunarizine (Flu). Each point is the average of six to ten experiments and the vertical bar gives the S.E.M.

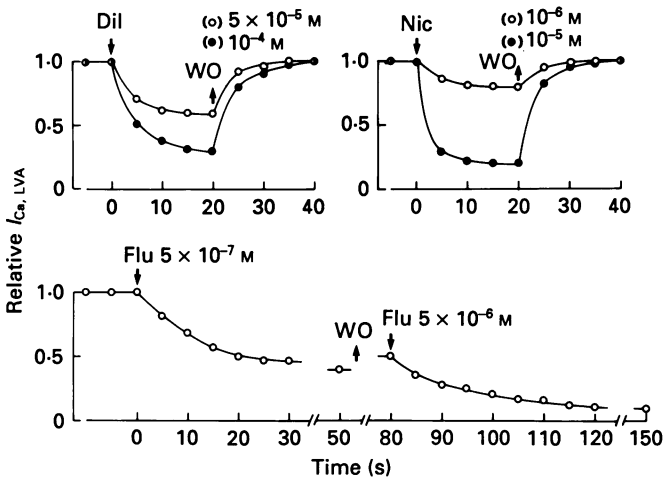


Fig. 9. Time courses of the effect of organic $Ca^{2+}$ channel antagonists on the low-threshold $Ca^{2+}$ current. Effects of diltiazem (Dil), nicardipine (Nic) and flunarizine (Flu) were examined on different neurones. Duration of drug application is indicated above the graphs. WO indicates the wash-out of the drug. $V_H$ was −100 mV and the currents were evoked by a voltage step to −30 mV.

effect of Bay K 8644 was observed. On the contrary, Bay K 8644 at concentrations above $1 \times 10^{-5}$ M exerted an inhibitory action.

The time course and reactivity of the channel blockade by organic $Ca^{2+}$ antagonists were also studied, under the same conditions; i.e. voltage steps from $-100$ to $-30$ mV, electrical stimulation every 5 s. The blocking effect appeared most rapidly when the dihydropyridine derivatives were used and it was completely reversible.

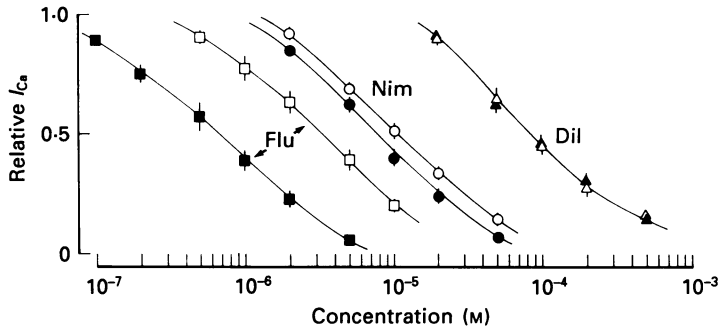


Fig. 10. Blockade of low- and high-threshold $Ca^{2+}$ currents by flunarizine (Flu), nimodipine (Nim) and diltiazem (Dil). The low- and high-threshold $Ca^{2+}$ currents were evoked by voltage steps to $-30$ mV from a $V_H$ of $-100$ mV and to 0 mV from a $V_H$ of $-60$ mV, respectively. Electrical stimulation was given every 5 s. (Filled symbols, low-threshold $Ca^{2+}$ currents; open symbols, high-threshold $Ca^{2+}$ currents.) The points are the means of six to eight experiments and the bars indicate S.E.M.

The effect of diltiazem developed somewhat more slowly. The time course of the inhibitory effect of flunarizine appeared slowly and was partly reversible (Fig. 9). The flunarizine blockade was enhanced when the low-threshold $Ca^{2+}$ channels had been previously inactivated by a long-lasting depolarization in the presence of the drug, thereby indicating that flunarizine has a voltage-dependent inhibitory action.

For comparison, some measurements were made on both the high-threshold and the low-threshold $Ca^{2+}$ inward currents. The high-threshold $Ca^{2+}$ currents were induced by a step voltage to 0 mV from a $V_H$ of $-60$ mV every 5 s. The blocking effects of nimodipine and especially of flunarizine were less evident, and the corresponding $K_D$s were $1 \times 10^{-5}$ M for nimodipine and $3{\cdot}2 \times 10^{-6}$ M for flunarizine. Diltiazem had the same inhibitory action on both low- and high-threshold $Ca^{2+}$ currents (Fig. 10). Tetrodotoxin up to $10^{-5}$ M had no effect on the low-threshold $Ca^{2+}$ current.

When the preparations were stimulated every 30 s, flunarizine, nimodipine and D600 produced a use-dependent decrease in current amplitude. The sequence of inhibitory action was in the order of flunarizine > nimodipine > D600. At stimulations every 1 and 5 s, however, diltiazem also induced a use-dependent inhibition. The use-dependent inhibition of flunarizine was considerably augmented with increasing stimulus frequency; i.e. the apparent $K_D$ values were $5 \times 10^{-6}$, $7 \times 10^{-7}$ and $9 \times 10^{-8}$ M at stimulations every 30, 5 and 1 s respectively.

## DISCUSSION

The kinetic characteristics of the low-threshold $Ca^{2+}$ current recorded from hypothalamic neurones are identical to those of the 'T-type' current in the chick, rat and mouse dorsal root ganglion (DRG) neurones (Carbone & Lux, 1987; Fox, Nowycky & Tsien, 1987*a*, *b*; Kostyuk, Shuba & Savchenko, 1987). The current activated at potentials above −65 mV reaches its peak in a highly potential-dependent manner. The occurence of fast inactivation is also potential dependent; it develops mainly in the potential range in which no $Ca^{2+}$ inward current can be evoked. Thus, any $Ca^{2+}$ influx into the cell as the cause of channel inactivation can be ruled out. As in the case of the DRG cells (Carbone & Lux, 1987), the recovery from inactivation also depends on the repolarizing potential level. The time constant decreases by a factor of three when the repolarizing potential level ($V_t$) is increased from −80 to −120 mV (see Fig. 5).

The ionic dependence of the low-threshold $Ca^{2+}$ channel of isolated hypothalamic neurones resembles that observed in peripheral neurones. The current dependence upon $[Ca^{2+}]_o$ shows a definite saturation which is quantitatively similar to that described by Carbone & Lux (1987). When $Ba^{2+}$ was substituted for $Ca^{2+}$, it produced a smaller or almost equal inward current as observed in rat and chick DRG neurones (Carbone & Lux, 1987; Fox *et al.* 1987*b*) and cultured hippocampal neurones from fetal rat (Yaari, Hamon & Lux, 1987), in contrast to what is known of the effect of such substitution on high-threshold $Ca^{2+}$ channels (Hagiwara & Ohmori, 1982; Akaike, Nishi & Oyama, 1983). This peculiarity may not reflect a genuine difference in the structure of the 'selectivity filter' of different types of $Ca^{2+}$ channels, but it may reflect a difference in the effect of $Ba^{2+}$ on $Ca^{2+}$ channel gating. It has recently been shown that $Ba^{2+}$ substituted for $Ca^{2+}$ decreases the mean open time of low-threshold $Ca^{2+}$ channels by a factor of about two. This effect may be negligible in high-threshold $Ca^{2+}$ channels because the mean open time is several times shorter (Shirokov, 1988).

In neuroblastoma cells (Narahashi *et al.* 1987) or DRG cells (Fox *et al.* 1987*a*), low-threshold $Ca^{2+}$ channels can be distinguished from high-threshold $Ca^{2+}$ channels by their differential sensitivities to $Cd^{2+}$ or $Ni^{2+}$; they are more resistant to $Cd^{2+}$ (2 or $3 \times 10^{-5}$ M induced only a small depression) whereas they are more sensitive to $Ni^{2+}$ ($1 \times 10^{-4}$ M largely abolished the current). On the other hand, both the low- and high-threshold $Ca^{2+}$ channels of cultured rat hippocampal neurones were completely suppressed by adding $10^{-4}$ M-$Cd^{2+}$ (Yaari *et al.* 1987). This may not be the case in hypothalamic neurones in which $10^{-4}$ M-$Cd^{2+}$ inhibited slightly the low-threshold $Ca^{2+}$ channels and the inhibition was somewhat stronger than with $Ni^{2+}$. More effective inhibition was observed by adding $Zn^{2+}$ and especially $La^{3+}$. The latter blocked low-threshold $Ca^{2+}$ currents with a $K_D$ of $7 \times 10^{-7}$ M. Such effective blocking of $Ca^{2+}$ channels by $La^{3+}$ has been noted in neuroblastoma cells for both types of channels (Narahashi *et al.* 1987).

The most striking feature of the low-threshold $Ca^{2+}$ channel in the hypothalamic neurones is their extreme sensitivity to organic $Ca^{2+}$ channel blockers. The channel could be blocked by all three representative groups of $Ca^{2+}$ channel antagonists such as verapamil, dihydropyridine and diltiazem derivatives. Members of the second group (nimodipine, nifedipine and nicardipine) acted with $K_D$s of several micromolar.

The dihydropyridine compound Bay K 8644, a $Ca^{2+}$-channel agonist, was also shown to be an effective channel blocker. Conversely, in experiments on both DRG neurones and cardiac cells, little sensitivity of low-threshold $Ca^{2+}$ channels to compounds such as nifedipine and related dihydropyridines has been repeatedly stressed (Nilius *et al.* 1985; Fox *et al.* 1987*a*). In avian DRG neurones, the low-threshold $Ca^{2+}$ current was depressed by Bay K 8644 while nifedipine was weakly agonistic or ineffective (Boll & Lux, 1985).

The most potent organic blocker of the low-threshold $Ca^{2+}$ channel in brain neurones proved to be flunarizine – a substance which has been shown to block contraction and inward $Ca^{2+}$ currents in intestinal and vascular smooth muscle cells. The affinity of this substance in muscle cells was not high ($K_D$ about $10^{-6}$ M), and the action developed slowly in a voltage- and use-dependent manner (Nagao, Suzuki & Kuriyama, 1986; Terada, Ohya, Kitamura & Kuriyama, 1987; Itoh, Satoh, Ishimatsu, Fujiwara & Kanmura, 1987). To our knowledge, flunarizine has never been tested on $Ca^{2+}$ channels in brain neurones which have just been isolated from young animals. As in the case of smooth muscle cells, the inhibitory effects of flunarizine on transmural stimulation-induced electrical and mechanical responses developed more slowly than did effects seen with verapamil, diltiazem and dihydropyridine derivatives (Nagao *et al.* 1986) and the inhibitory effect was hardly reversible (Terada *et al.* 1987).

Concerning the possible role of the low-threshold $Ca^{2+}$ current in brain neurones, its presence is assumed to be a constant feature in hypothalamic neurones. Such may be the case in other types of brain neurones, according to the current-clamp analysis by Llinás & Yarom (1981*a*, *b*). The relative density of this current (compared with that of the high-threshold one) is high and in many cells the low-threshold $Ca^{2+}$ current is dominant. In DRG neurones the situation is different: a distinct low-threshold $Ca^{2+}$ current can be found only in some cells, and the density is usually much lower than that of the high-threshold current. At embryonic or early postnatal stages, a low-threshold $Ca^{2+}$ current dominates over a high-threshold current. Thus, in the DRG neurones, low-threshold $Ca^{2+}$ channels may be considered more as a feature of the membrane of developing neurones rather than structures important for the function of mature ones (Carbone & Lux, 1984*a*; Kostyuk *et al.* 1986).

In brain neurones, the low-threshold $Ca^{2+}$ conductance should play an important role in functions by contributing to spontaneous depolarization waves and rebound excitation. As we have constantly recorded this type of conductance in isolated neurones which lacked terminal dendrite branches, the low-threshold $Ca^{2+}$ channels seem to be present in the somatic membrane. However, it should be kept in mind that when isolating cells from brain tissue there are remaining dendritic processes. Therefore, the partial contribution of dendritic membrane to the low-threshold $Ca^{2+}$ current recorded cannot be ruled out.

Our data provide new approaches for studying the effects of organic $Ca^{2+}$ channel agonists and antagonists on neuronal functions of the central nervous system. The potent inhibitory action of dihydropyridine derivatives and flunarizine on low-threshold $Ca^{2+}$ channels will facilitate a precise analysis of brain functions, at the molecular level, and also a search for practical uses of organic $Ca^{2+}$ channel blockers in the treatment of neurological diseases.

We thank Drs M. Yoshii, R. Llinás and M. Ohara for their pertinent comments. This study was funded by Grants-in-Aid to N. Akaike from the Ministry of Education, Science and Culture Nos. 62870102, 63480107 and 63641526, the Brain Science Foundation, and the Japan Foundation for Health Sciences.

## REFERENCES

AKAIKE, N., INOUE, M. & KRISHTAL, O. A. (1986). 'Concentration clamp' study of γ-aminobutyric-acid-induced chloride current kinetics in frog sensory neurones. *Journal of Physiology* **379**, 171–185.

AKAIKE, N., NISHI, K. & OYAMA, Y. (1983). Characteristics of manganese current and its comparison with currents carried by other divalent cations in snail soma membranes. *Journal of Membrane Biology* **76**, 289–297.

AKAIKE, N., YAKUSHIJI, T., TOKUTOMI, N. & CARPENTER, D. O. (1987). Multiple mechanisms of antagonism of γ-aminobutyric acid (GABA) responses. *Cellular and Molecular Neurobiology* **7**, 97–103.

ARMSTRONG, C. M. & MATTESON, D. R. (1985). Two distinct populations of calcium channels in a clonal line of pituitary cells. *Science* **227**, 65–67.

BEAN, B. P. (1985). Two kinds of calcium channels in canine atrial cells. *Journal of General Physiology* **86**, 1–31.

BEAN, B. P., STUREK, M., PUGA, A. & HERMSMEYER, K. (1985). Calcium channels in smooth muscle cells from mesenteric arteries. *Journal of General Physiology* **86**, 23a.

BOLL, W. & LUX, H. D. (1985). Action of organic antagonists on neuronal calcium currents. *Neuroscience Letters* **56**, 335–339.

BOSSU, J. L., FELTZ, A. & THOMANN, J. M. (1985). Depolarization elicits two distinct calcium currents in vertebrate sensory neurones. *Pflügers Archiv* **403**, 360–368.

CARBONE, E. & LUX, H. D. (1984*a*). A low-voltage activated calcium conductance in embryonic chick sensory neurons. *Biophysical Journal* **46**, 413–418.

CARBONE, E. & LUX, H. D. (1984*b*). A low voltage-activated fully inactivating Ca channel in vertebrate sensory neurones. *Nature* **310**, 501–502.

CARBONE, E. & LUX, H. D. (1987). Kinetics and selectivity of a low-voltage-activated calcium current in chick and rat sensory neurones. *Journal of Physiology* **386**, 547–570.

COHEN, C. J. & MCCARTHY, R. T. (1985). Different effects of dihydropyridines on two populations of Ca channels in anterior pituitary cells. *Biophysical Journal* **47**, 513a.

FEDULOVA, S. A., KOSTYUK, P. G. & VESELOVSKY, N. S. (1985). Two types of calcium channels in the somatic membrane of new-born rat dorsal root ganglion neurones. *Journal of Physiology* **359**, 431–446.

FOX, A. P., NOWYCKY, M. C. & TSIEN, R. W. (1987*a*). Kinetics and pharmacological properties distinguishing three types of calcium currents in chick sensory neurones. *Journal of Physiology* **394**, 149–172.

FOX, A. P., NOWYCKY, M. C. & TSIEN, R. W. (1987*b*). Single-channel recordings of three types of calcium channels in chick sensory neurones. *Journal of Physiology* **394**, 173–200.

GRAY, R. & JOHNSTON, D. (1986). Multiple types of calcium channels in acutely-exposed neurons from adult hippocampus. *Biophysical Journal* **49**, 432a.

HAGIWARA, S. & OHMORI, H. (1982). Studies of calcium channels in rat clonal pituitary cells with patch electrode voltage clamp. *Journal of Physiology* **331**, 231–252.

ITOH, T., SATOH, S., ISHIMATSU, T., FUJIWARA, T. & KANMURA, Y. (1987). Mechanism of flunarizine-induced vasodilatation in the rabbit mesenteric artery. *Circulation Research* **61**, 446–454.

KANEDA, M., NAKAMURA, H. & AKAIKE, N. (1988). Mechanical and enzymatic isolation of mammalian CNS neurones. *Neuroscience Research* **5**, 299–315.

KOSTYUK, P. G., FEDULOVA, S. A. & VESELOVSKY, N. S. (1986). Changes in ionic mechanisms of electrical excitability of the somatic membrane of rat dorsal root ganglion neurons during ontogenesis. Distribution of ionic channels of inward current. *Neurophysiology (Kiev)* **18**, 813–820.

KOSTYUK, P. G., SHUBA, M. F. & SAVCHENKO, A. N. (1987). Three types of calcium channels in the membrane of mouse sensory neurones. *Biological Membranes (Moscow)* **4**, 366–373.

LLINÁS, R. & YAROM, Y. (1981*a*). Electrophysiology of mammalian inferior olivary neurones *in vitro*. Different types of voltage-dependent ionic conductances. *Journal of Physiology* **315**, 549–567.

LLINÁS, R. & YAROM Y. (1981*b*). Properties and distribution of ionic conductances generating electroresponsiveness of mammalian inferior olivary neurones *in vitro*. *Journal of Physiology* **315**, 569–584.

MITRA, R. & MORAD, M. (1986). Two calcium channels in guinea-pig ventricular myocytes. *Proceedings of the National Academy of Sciences of the USA* **93**, 5340–5344.

NAGAO, T., SUZUKI, H. & KURIYAMA, H. (1986). Effects of flunarizine on electrical and mechanical responses of smooth muscle cells on basilar and ear arteries of the rabbit. *Naunyn Schmiedeberg's Archives of Pharmacology* **333**, 431–438.

NARAHASHI, T., TSUNOO, A. & YOSHII, M. (1987). Characterization of two types of calcium channels in mouse neuroblastoma cells. *Journal of Physiology* **383**, 231–249.

NILIUS, B., HESS, P., LANSMAN, J. B. & TSIEN, R. W. (1985). A novel type of cardiac calcium channel in ventricular cells. *Nature* **316**, 443–446.

OHMORI, H. & YOSHII, M. (1977). Surface potential reflected in both gating and permeation mechanisms of sodium and calcium channels of the tunicate egg cell membrane. *Journal of Physiology* **267**, 429–463.

PORTZEHL, H., CALDWELL, P. C. & RÜEGG, J. C. (1964). The dependence of contraction of muscle fibres from the crab *Maia squinado* on the internal concentration of free calcium ions. *Biochimica et biophysica acta* **79**, 581–591.

SHIROKOV, R. E. (1988). Potential dependence of calcium current deactivation in the somatic membrane of mouse sensory neurons. *Neurophysiology (Kiev)* **20**, 185–192.

STUREK, M. & HERMSMEYER, K. (1986). Two different types of calcium channels on spontaneously contracting vascular smooth muscle cells. *Journal of General Physiology* **86**, 23a.

TERADA, K., OHYA, Y., KITAMURA, K. & KURIYAMA, H. (1987). Actions of flunarizine, a $Ca^{2+}$ antagonist, on ionic currents in fragmented smooth muscle cells of the rabbit small intestine. *Journal of Pharmacology and Experimental Therapeutics* **240**, 978–983.

VESELOVSKY, N. S. & FEDULOVA, S. A. (1982). Two types of calcium channels in the somatic membrane of rat spinal ganglion neurons. *Proceedings of the USSR Academy of Sciences* **268**, 747–750.

YAARI, Y., HAMON, B. & LUX, H. D. (1987). Development of two types of calcium channels in cultured mammalian hippocampal neurons. *Science* **235**, 680–682.